Appl. Magn. Reson. 26, 223–244 (2004)

Applied Magnetic Resonance

Data Analysis Procedures for Pulse ELDOR Measurements of Broad Distance Distributions

G. Jeschke[1], G. Panek[1], A. Godt[2], A. Bender[3], and H. Paulsen[3]

[1] Max Planck Institute for Polymer Research, Mainz, Germany
[2] Fakultät für Chemie, Universität Bielefeld, Bielefeld, Germany
[3] Institut für Allgemeine Botanik, Universität Mainz, Mainz, Germany

Received September 25, 2003

Abstract. The reliability of procedures for extracting the distance distribution between spins from the dipolar evolution function is studied with particular emphasis on broad distributions. A new numerically stable procedure for fitting distance distributions with polynomial interpolation between sampling points is introduced and compared to Tikhonov regularization in the dipolar frequency and distance domains and to approximate Pake transformation. Distance distributions with only narrow peaks are most reliably extracted by distance-domain Tikhonov regularization, while frequency-domain Tikhonov regularization is favorable for distributions with only broad peaks. For the quantification of distributions by their mean distance and variance, Hermite polynomial interpolation provides the best results. Distributions that contain both broad and narrow peaks are most difficult to analyze. In this case a high signal-to-noise ratio is strictly required and approximate Pake transformation should be applied. A procedure is given for renormalizing primary experimental data from protein preparations with slightly different degrees of spin labelling, so that they can be compared directly. Performance of all the data analysis procedures is demonstrated on experimental data for a shape-persistent biradical with a label-to-label distance of 5 nm, for a [2]catenane with a broad distance distribution, and for a doubly spin-labelled double mutant of plant light harvesting complex II.

1 Introduction

Pulse electron paramagnetic resonance (EPR) experiments [1] on spin probes and spin labels can provide precise distances between selected sites in complex materials in the 2–5 nm range and in favorable cases in the 1.6–8 nm range [2]. Since few alternative techniques exist for such measurements on systems that lack long-range order, these methods have recently been applied in a number of studies on synthetic macromolecules and supramolecular structures [3–6]. The combination with site-directed spin-labelling [7, 8] is very promising for the structural characterization of proteins by long-range distance constraints [9].

Among the currently used experiments [2, 10–16] pulse electron-electron double resonance (ELDOR) experiments are particularly simple to analyze theoretically, as the signal for multispin systems factorizes into pair contributions [11, 12, 17, 18]. If angular correlations between spin-to-spin vectors and effects of orientation selection [19] can be neglected, the dipolar evolution function measured by such experiments is thus directly related to the spin-spin pair correlation function. Therefore, even broad distance distributions can be characterized, at least if a reasonable model of the structure exists [6]. Such relatively broad distance distributions have also been encountered for aggregates of polypeptides [20, 21] and in our own, hitherto unpublished measurements on membrane proteins, where a model-free conversion of the dipolar evolution function to the distance distribution $P(r)$ would be advantageous [17, 18]. It is well known that the Pake transformation, which underlies such a model-free conversion, corresponds to an ill-posed problem, so that moderate noise can already cause significant artefacts in $P(r)$. In other words, in the presence of some noise, a good fit of the experimental data set by a distance distribution does not necessarily guarantee that all the features of this distribution are real. This problem is expected to be more cumbersome for broad distributions than for the narrow distributions that have been mainly studied to date. At the current level of knowledge, it is difficult to estimate the reliability of broad distributions extracted from experimental data.

Here we present a comparative study of different approaches for extracting the distance distribution $P(r)$ from the dipolar time evolution function $V(t)$. We consider the width of peaks in the distance distribution, the presence of noise, and the maximum time t_{max} in the measurement of $V(t)$. After a short review of analytical expressions for $V(t)$ we derive expressions for the case of dilute clusters of spins. On the basis of these expressions we discuss the separation of the background contribution stemming from remote spins in different clusters from the contribution stemming from spins in one cluster. We then describe a procedure for modulation depth renormalization that can distinguish differences in experimental dipolar evolution functions which are merely due to different degrees of spin labelling from differences that are due to changes in $P(r)$. After a short discussion of the limitations of approximate Pake transformation (APT) [17, 18] and Tikhonov regularization [22–24] we introduce an iterative fitting procedure that is based on piecewise Hermite polynomial interpolation of $P(r)$ between sampling points. We then discuss the reduction of information on $P(r)$ to a few characteristic parameters by moment analysis and define descriptive width parameters of the distribution. The different approaches are then compared for several model distance distributions by analysing simulated dipolar evolution functions that are superimposed by white noise. Finally, experimental data are analyzed for a shape-persistent biradical with a label-to-label distance of 5 nm [25], a [2]catenane [6], and a double mutant of plant light harvesting complex II (LHCII) reconstituted with different single xanthophyll components next to chlorophyll *a* and *b*.

2 Materials and Methods

Synthesis of the shape-persistent biradical [25] and of the doubly spin-labelled [2]catenane [6, 26] have been described earlier. The double mutant S106C/S160Ch of the LHCII apoprotein was dissolved (1 mg/ml) in an aqueous solution of sodium dodecyl sulfate (0.5 weight%) and sodium phosphate buffer of pH 7 (20 mM). Reduction of any present disulfide linkages to free SH groups was achieved by incubation with tris-(2-carboxyethyl)phosphine (TCEP, 2 mM) for 2 h. Spin labelling was performed by adding 4-(2-iodoacetamido)-2,2,6,6-tetramethylpiperidine 1-oxyl (Sigma-Aldrich, tenfold molar excess) and incubating over night at ambient temperature on a shaker. The protein was then precipitated by addition of 100 mM acetic acid (1/10 of the original volume) and acetone (2.3 times the original volume). After centrifugation the protein was washed several times with 70% ethanol/30% water and once with absolute ethanol. The protein pellet was dried for 15 min at ambient temperature. This doubly labelled protein was then used in reconstitution of LHCII following a standard procedure [27].

Dipolar time evolution data were obtained at X-band frequencies (of about 9.3–9.4 GHz) on a Bruker Elexsys 580 spectrometer equipped with a Bruker Flexline split-ring resonator ER 4118X_MS3 using the four-pulse DEER experiment $\pi/2(\nu_{obs})-\tau_1-\pi(\nu_{obs})-t'-\pi(\nu_{pump})-(\tau_1+\tau_2-t')-\pi(\nu_{obs})-\tau_2-$echo [13]. The dipolar evolution time in this experiment is $t = t' - \tau_1$. Data were analyzed only for $t > 0$. The resonator was overcoupled to Q of about 100, the pump frequency ν_{pump} was set to the center of the resonator dip and coincided with the maximum of the nitroxide EPR spectrum, while the observer frequency ν_{obs} was 65 MHz higher and coincided with the low-field local maximum of the spectrum. Measurements on the shape-persistent biradical and the [2]catenane were performed at a temperature of 15 K with a pump pulse length of 32 ns, while measurements on LHCII reconstituted with the doubly spin-labelled double mutant S106C/S160Ch were performed at a temperature of 50 K with a pump pulse length of 12 ns. Proton modulation was averaged by adding traces at 25 different τ_1 values, starting at $\tau_1(0) = 200$ ns and incrementing by $\Delta\tau_1 = 8$ ns.

Tikhonov regularization with optimum choice of the regularization parameter was performed with the program FTIKREG [23, 24] by implementing routines for the computation of dipolar evolution functions $V(t, \omega_{dd})$ for given dipolar frequency ω_{dd} or distance r in the Fortran source code (subroutine KTISJ1, see appendix). Computation of pair correlation functions by direct transformation [17] and by cubic Hermite interpolation between sampling points as described below was accomplished with home-written Matlab programs. The source codes are available at http://www.mpip-mainz.mpg.de/~jeschke/distance.html. Distance-domain smoothing with a filter width of 0.1 nm was applied to APT results unless noted otherwise.

3 Computational Procedures

3.1 Dipolar Evolution Function for Dilute Clusters

Many applications of EPR distance measurements are concerned with dilute biradicals or dilute doubly labelled biomacromolecules. In this case the primary signal of a pulse ELDOR experiment normalized to unity at time $t = 0$ (dipolar evolution function $V(t)$) can be written as the product of an intramolecular part V_{pair} and an intermolecular part V_{hom} stemming from homogeneously distributed remote spins [12]. The intermolecular part corresponds to an exponential decay whose time constant depends on the concentration c and the fraction λ of spins that are inverted by the pump pulse

$$V_{\mathrm{hom}}(t,c) = \exp\left(-\frac{2\pi g^2 \mu_{\mathrm{B}}^2 \mu_0 N_{\mathrm{A}}}{9\sqrt{3}\hbar}\lambda ct\right),$$

where g is the g value of the two electron spins (differences between the two g values are assumed to be negligible), μ_{B} is the Bohr magneton, and N_{A} the Avogadro constant. For a fixed distance r of the spin pair, the intramolecular part is given by

$$V_{\mathrm{pair}}(t,r) = 1 - \lambda + \lambda \int_0^{\pi/2} \cos\left[(1 - 3\cos^2\theta)\omega_{\mathrm{dd}}(r)t\right]\sin\theta \mathrm{d}\theta, \tag{1}$$

where we have assumed that λ does not depend on the angle θ between the external field and the spin-spin vector in the pair and where the distance dependence of the dipolar frequency is described by

$$\omega_{\mathrm{dd}}(r) = \frac{1}{r^3}\frac{\mu_0 g^2 \mu_{\mathrm{B}}^2}{4\pi\hbar}. \tag{2}$$

As is apparent from Eq. (1), λ can be considered as a modulation depth for an isolated pair. For a distribution of distances in the pair, described by the pair correlation function $G(r)$, Eq. (1) can be integrated over r. As we have shown recently, the restriction to dilute spin pairs can be overcome when the angular correlation between spin-spin vectors of several coupled spins is negligible [17, 18]. In this situation there is a unique mapping between $G(r)$ and the dipolar evolution function and the signal can be computed as the product of contributions from infinitely thin spherical shells. With this result, we obtain the dipolar evolution function of a sample consisting of dilute clusters of radicals

$$\ln V(t) = -\lambda\left\{\overline{n} - 1 + \frac{2\pi g^2 \mu_{\mathrm{B}}^2 \mu_0 N_{\mathrm{A}}}{9\sqrt{3}\hbar}ct\right.$$

$$- \int_{r_{min}}^{r_{max}} 4\pi r^2 G_{cluster}(r) \int_0^{\pi/2} \cos\left[(1-3\cos^2\theta)\omega_{dd}t\right]\sin\theta \mathrm{d}\theta \mathrm{d}r \Bigg\}, \quad (3)$$

where $\bar{n}$ is the average number of radicals in a cluster, and where the cluster-only part of the spin-spin pair correlation function $G_{cluster}$ is normalized:

$$\int_{r_{min}}^{r_{max}} 4\pi r^2 G_{cluster}(r)\mathrm{d}r = \bar{n} - 1.$$

For a negligible homogeneous decay contribution, the modulation depth for clusters is $\lambda(\bar{n} - 1)$, as was pointed out earlier by Milov et al. [11].

The lower integration limit r_{min} in Eq. (3) depends on the excitation band width and hence on the pulse length. For the experimental conditions used in this work, $r_{min} = 1.5$ nm is a reasonable choice [17, 18]. The upper integration limit generally depends on the maximum observation time t_{max}, as effects from more remote spins are increasingly significant with increasing time t. For maximum observation times of 8 μs, $r_{max} = 40$ nm is a safe choice. However, in the case at hand the effective limit is set by the size of the clusters, which may for instance be aggregates of biomacromolecules. Doubly labelled proteins or protein complexes can be considered as a special case of clusters with $\bar{n} = 2$. For such samples r_{max} corresponds to the maximum expected distance between the labels. For the discussion of label-to-label separations, the distance distribution

$$P(r) = 4\pi r^2 G_{cluster}(r)$$

is most convenient.

According to Eq. (3), linear baseline correction of the logarithm of the signal provides the term that is solely due to spin pairs within the same cluster. The exponential of this term, renormalized to unity at $t = 0$, is a cluster-only dipolar evolution function $V_{cluster}(t)$ corresponding to an ideal measurement on isolated clusters with full modulation of the echo. When extracting $V_{cluster}(t)$ from experimental data, a range for the linear baseline fit must be selected. Usually the long-time behavior is dominated by the background contribution, so that the optimum range corresponds to $t_{bckg} < t < t_{max}$. For narrow distributions, visual inspection of the data yields a good estimate for t_{bckg} and, furthermore, the result does not depend strongly on the particular choice. For broad distributions or distances longer than about 4 nm, an automatic, adaptive choice of t_{bckg} is more suitable. For this, we perform APT [17] for all possible values of t_{bckg} in the range between $0.1t_{max}$ and $0.9t_{max}$. The best background correction should yield a distance distribution $P(r)$ that decays to zero at long distances. We thus select the value of t_{bckg} at which $|P(r_{max,APT})|$ is minimum, where $r_{max,APT}$ is the upper distance limit of the APT for the given dataset.

Extraction of $G_{cluster}(r)$ or $P(r)$ from $V_{cluster}(t)$ is generally an ill-posed (or ill-conditioned) problem, in which small statistical variations (noise) in the input function $V_{cluster}(t)$ may cause strong variations in the output function $P(r)$. To a certain degree, this problem can be mended by an integral transformation with properly selected digital resolution in the dipolar frequency domain, mapping to distance domain, and subsequent distance domain smoothing [17].

Alternatively, Tikhonov regularization [22] with adaptive choice of the regularization parameter [23, 24] can be used [18; P. P. Borbat and J. H. Freed, Cornell University, Ithaca, NY, USA, pers. commun.]. For the similar problem of extracting dipolar frequencies from rotational echo double resonance (REDOR) data in solid-state nuclear magnetic resonance (NMR), a study concerning distance distributions with only narrow peaks found that Tikhonov regularization is advantageous for noisy data [28]. In the following we mainly consider the case of distance distributions containing broad peaks, as they are typical for membrane proteins labelled in the loop regions.

3.2 Comparison of Data Sets

Site-directed spin labelling (SDSL) is often used to reveal function-related structural changes in biomacromolecules [7, 8, 29]. For this purpose it would be useful to reliably detect small changes in the distance distribution $P(r)$. We have encountered the same problem in the characterization of LHCII samples that are reconstituted with different xanthophylls or in the presence of different lipids. As extraction of $P(r)$ is an ill-posed problem, apparently significant differences in the experimental distance distribution of two samples may result from moderate noise, as we shall also see in the Sect. 4. Therefore, direct comparison of the primary time-domain data reveals more clearly whether the differences between two samples are statistically significant.

To test reproducibility for like samples, we have performed measurements with careful adjustment of all parameters of the four-pulse DEER experiment on several samples prepared by the same procedure from the same constituents. We have found that primary experimental data for such nominally identical samples often vary in the modulation depth λ. The most likely cause is variation in the efficiency of spin labelling, leading to slightly different ratios of doubly labelled to singly labelled protein. For repeated measurements on the same sample we find smaller, but still noticeable, variations in λ that are presumably due to unavoidable small differences in the width and shape of the cavity mode, which in turn lead to slightly different excitation profiles of the pulses.

As we are interested only in changes in the "true" pair correlation function, we need to compensate for these variations in λ. From Eq. (3) it follows that a mere difference in the modulation depth λ between two samples corresponds to scaling of the logarithm of the primary data $V(t)$ by a constant factor $f_\lambda = \lambda_1/\lambda_2$. Assume that two data sets $V_1(t_k)$ and $V_2(t_k)$ are specified at N discrete times t_k. The experimental scaling factor

$$f_\lambda = \frac{\sum_{k=1}^{N} [\ln V_1(t_k)]^2}{\sum_{k=1}^{N} \ln V_1(t_k) \ln V_2(t_k)}$$

corresponds to a minimum root mean square difference between $\ln V_1$ and $f_\lambda \ln V_2$. The difference signal,

$$\Delta V = \exp(f_\lambda \ln V_2) - V_1$$

is thus a measure for differences in the spin-spin pair correlation function between the two samples. Differences in the modulation depths caused by slightly different spectrometer settings do not contribute to ΔV. A different ratio of singly labelled to doubly labelled protein molecules may influence the relative weights of the homogeneous contribution and the cluster contribution on the right-hand side of Eq. (3) and thus may not be fully compensated by the scaling. However, in measurements on proteins one usually works at concentrations where the homogeneous contribution is the smallest of the three terms on the left-hand side of Eq. (3), so that moderate changes in the ratio of cluster concentration to bulk concentration of the spin labels are not expected to cause a significant contribution to ΔV.

3.3 Iterative Fitting of a Model-Free Pair Correlation Function

In our previous derivation of the APT procedure for extracting $G(r)$ from dipolar time evolution data, we discretized the dipolar frequency domain in a way that approximately minimized the condition number of the crosstalk matrix [17]. We obtained condition numbers of about 3, indicating that for this discretization the problem is reasonably well-posed. Yet, scaling of the dipolar evolution function with t in this approach decreases the signal-to-noise ratio and any condition number larger than unity means that noise introduces some crosstalk, i.e., some interference between values of $P(r)$ at different r. Our recent experience with broad distance distributions in doubly spin-labelled [2]catenanes [6] has shown that this may introduce unreasonably narrow features into the experimental $P(r)$. These artefacts can be eliminated by distance-domain smoothing only at the price of undue broadening of the true features.

For any given data set there is a resolution in distance domain which is an optimum compromise between the appearance of such crosstalk artefacts and artificial broadening of $P(r)$. In principle, Tikhonov regularization with adaptive choice of the regularization parameter is supposed to automatically provide this optimum resolution [23, 24]. Furthermore, unlike APT, Tikhonov regularization can incorporate the constraint $P(r) \geq 0$, which is known to counteract the appearance of crosstalk artefacts. However, our experience shows that for broad distance distributions, this technique tends to yield $P(r)$ consisting of a multitude of narrow peaks if distance-domain data are computed directly (see Sect.

4). If data are first computed in dipolar frequency domain and then mapped to distances, narrow features may be lost in distributions that contain both narrow and broad peaks (see also Sect. 4). It is therefore desirable to study systematically how the appearance of artefacts in $P(r)$ and the deviation between experimental and simulated dipolar evolution functions depend on the selected resolution in distance domain.

For that purpose we model $P(r)$ by polynomial interpolation between n_s equidistant sampling points r_k in distance domain. The $P_k = P(r_k)$ are variables in a nonlinear fit procedure performed with the simplex algorithm. The dipolar time evolution function $V_{fit}(t)$ for the current model distance distribution is computed by shell factorization [17] and the best-fit P_k values are determined by minimizing the root mean square deviation of $V_{fit}(t)$ from $V_{cluster}(t)$ under the constraint $P_k \geq 0$. The cluster-only dipolar evolution function $V_{cluster}(t)$ in the range from $t = 0$ to $t = t_{max}$ is computed from experimental or simulated data as described in Sect 3.2. The use of piecewise cubic Hermite interpolation rather than spline interpolation between the sampling points ensures that the interpolated model distance distribution is nonnegative in between sampling points.

To enhance numerical stability and to avoid convergence to local minima, the fit procedure is started with only $n_s = 8$ sampling points r_k, with $r_1 = r_{min} = 1.75$ nm and $r_8 = r_{max}$. Here r_{max} is the distance obtained by Eq. (2) from the minimum detectable dipolar frequency $\omega_{dd,min} = 5\pi/(4t_{max})$ [17]. A good set of starting values for the P_k can be derived by direct transformation of $V_{cluster}(t)$ to the dipolar frequency domain, mapping to distance domain with Eq. (2), and distance domain smoothing with a Gaussian filter width of 0.5 nm.

To increase the resolution of the modelled distance distribution $P(r)$, an new set of r_k is defined by inserting additional sampling points halfway between the existing sample points. The starting values $P_{k,0}$ at these new sampling points are the values of the interpolating Hermite polynomial of the previous set of sampling points. Typically we perform five iterations of this procedure so that we obtain model distance distributions $P^{(1)}(r)...P^{(5)}(r)$ with $n_s = 8$, 15, 29, 57, and 113 sampling points between r_{min} and r_{max}. For the usually achievable observation times $t_{max} < 8$ μs this corresponds to a resolution of about 0.05 nm or better in the last step. Higher resolution is unrealistic as conformational distributions irrevocably cause larger peak widths than that in $P(r)$ even for shape-persistent molecules [25]. Improvements in the quality of the fits with increasing resolution of $P(r)$ can be assessed by changes in the r.m.s. deviation of $V_{fit}(t)$ from $V_{cluster}(t)$.

3.4 Characteristic Parameters of Broad Distance Distributions

In the presence of moderate or strong noise, different data analysis procedures may provide significantly different distance distributions $P(r)$, since the problem of extracting $P(r)$ from $V_{cluster}(t)$ is generally ill-posed. Nevertheless, certain characteristics of $P(r)$, such as its mean value and variance, may be defined with high or at least satisfying precision by the available experimental data. For the

distribution of ionic spin probes in telechelic ionomers, we could determine such characteristic parameters by fitting a $P(r)$ consisting of one or two Gaussian peaks and a homogeneous background contribution [4, 5]. However, in the case of doubly-labelled LHCII, this approach was found to be numerically unstable. A model-free reduction of distributions to characteristic parameters can be achieved by moment analysis. The first moment,

$$\langle r \rangle = \frac{\int_{r_{min}}^{r_{max}} rP(r)\mathrm{d}r}{\int_{r_{min}}^{r_{max}} P(r)\mathrm{d}r},$$

is the mean distance. Higher moments of order $n > 1$ are defined by

$$\langle \Delta r^n \rangle = \frac{\int_{r_{min}}^{r_{max}} (r - \langle r \rangle)^n P(r)\mathrm{d}r}{\int_{r_{min}}^{r_{max}} P(r)\mathrm{d}r}.$$

The second moment or variance of the distribution, $\langle \Delta r^2 \rangle$, is of the order of the square of the width of the distribution, while the third moment, $\langle \Delta r^3 \rangle$, characterizes the asymmetry of the distribution. A more descriptive width parameter $\Gamma_{0.5}$ can be defined by

$$\frac{\int_{\langle r \rangle - \Gamma_{0.5}/2}^{\langle r \rangle + \Gamma_{0.5}/2} P(r)\mathrm{d}r}{\int_{r_{min}}^{r_{max}} P(r)\mathrm{d}r} = 0.5.$$

In other words, $\Gamma_{0.5}$ is the width of the range in which 50% of all spin-to-spin distances are found. Analogously, a parameter $\Gamma_{0.9}$ can be defined as the width in which 90% of all spin-to-spin distances are found.

4 Results

4.1 Assessing Structural Changes in LHCII

Data typical for the reproducibility of our measurements on doubly spin-labelled LHCII from different preparations are shown in Fig. 1. The data from independent measurements on the double mutant S106C/S160Ch of LHCII reconstituted with pure neoxanthin (NX) can be superimposed by scaling with a factor f_λ = 1.091 (Fig. 1a, c), while data from the measurements of the same double mutant reconstituted with pure zeaxanthin (ZX) can be superimposed with a factor f_λ = 1.631. In both cases, the difference between the superimposed traces is virtually pure white noise, except for small deviations close to t_{max} (arrows in Fig. 1c, d) that are caused by slightly different amplitudes of the residual proton

modulation. In contrast, traces of LHCII reconstituted with NX are not superimposable with traces of LHCII reconstituted with ZX (Fig. 1e, f). At shorter times, the decay of the normalised signal is faster for ZX, as is apparent from the negative difference signal in the range from about 0.2 to about 1.2 μs, whereas it is slower at longer times. This indicates a broader distance distribution for NX.

4.2 Extraction of Distance Distributions from Model Data Sets

For systems with well defined distances (one narrow peak in the distance distribution), no particular problems in data analysis are expected if the data can be acquired with good signal-to-noise ratio. This is borne out by analysis of the simulated data set (Fig. 2a) corresponding to a distance distribution with one Gaussian peak at 5 nm with a standard deviation of 0.2 nm. The four alternative approaches APT, Tikhonov regularization in frequency domain (Tikh.-ω_{dd}) and distance domain (Tikh.-r), and fitting by Hermite interpolating polynomial distributions (Poly-$P^{(n)}$) all give reasonable results. Approaches on the basis of a primary analysis in dipolar frequency domain (APT and Tikh.-ω_{dd}) have limited resolution. In principle, the resolution may be improved by zero-filling; but as the modulation has not decayed and as the effect of apodization in these techniques is not well understood, we have refrained from this. Note that despite the good signal-to-noise ratio, Poly-$P^{(4)}$ and Poly-$P^{(5)}$ display an apparent fine structure of the peak, which is an artefact. As is clearly seen in Fig. 2c, increasing the number of sampling points beyond $n_s = 29$ (Poly-$P^{(3)}$) does not strongly improve the fit. Moment analysis gives mean distances of 4.6 nm for Tikhonov regularization in frequency domain, 5.2 nm for APT, 4.9 nm for Poly-$P^{(1)}$ and the precise result of 5.0 nm for Tikhonov-regularization in distance domain as well as Hermite polynomial fitting with at least 15 sampling points (Poly-$P^{(2)}$ to Poly-$P^{(5)}$). For the standard deviation (square root of the second moment), Tikhonov regularization in distance domain gives a value of 0.40 nm, i.e., an overestimate by a factor of two. The best results for this parameter are obtained from the distributions Poly-$P^{(4)}$ (0.28 nm) and Poly-$P^{(5)}$ (0.25 nm).

As an example for an asymmetric distance distribution we have selected the Birnbaum-Saunders distribution originally introduced to model the lifetime distribution of materials subject to a physical fatigue process [30]. Results of exponential background correction and data analysis by the alternative approaches are displayed in Fig. 3a, b for two different signal-to-noise ratios. For this broad distribution, adaptive choice of the regularization parameter in distance domain Tikhonov regularization is not successful even at moderate noise amplitude (Fig. 3b, trace III). For the signal-to-noise ratio of the data displayed in Fig. 3c, the algorithm for finding the optimum regularization parameter fails altogether. In this situation, Tikhonov regularization in dipolar frequency domain provides the best result. Hermite polynomial fitting with a small number of sampling points and APT also perform reasonably well. Increasing the number of sampling points in

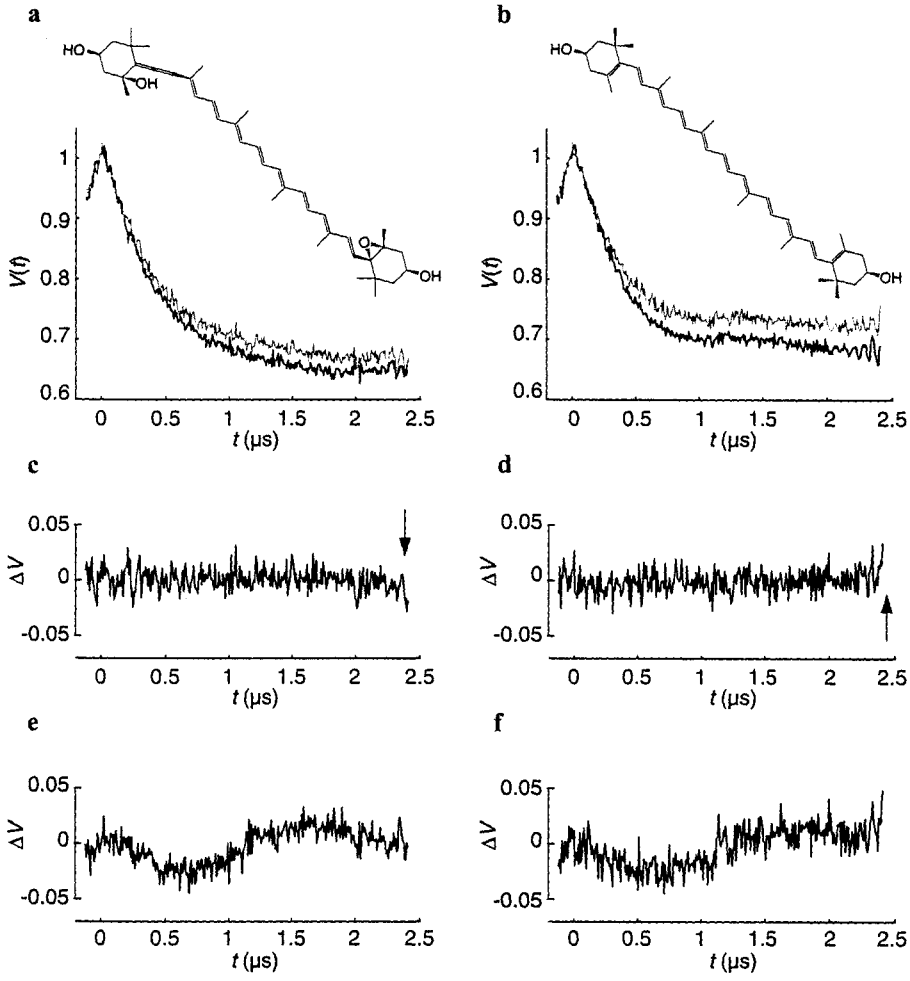

Fig. 1. Assessment of structural differences in LHCII reconstituted with the two different xanthophylls neoxanthin (NX) and zeaxanthin (ZX) by comparison of dipolar time evolution data (doubly spin-labelled double mutant S106C/S160Ch). Arrows in **c** and **d** mark small deviations caused by proton modulations (see text). **a** Primary experimental data for two different preparations of LHCII reconstituted with NX (inset). **b** Primary experimental data for two different preparations of LHCII reconstituted with ZX (inset). **c** Difference of the two traces in **a** after scaling with optimum f_λ = 1.091. **d** Difference of the two traces in **b** after scaling with optimum f_λ = 1.631. **e** Difference ZX-NX of the black traces in **a** and **b** after optimum scaling. **f** Difference ZX-NX of the grey traces in **a** and **b** after optimum scaling.

Hermite polynomial fitting from n_s = 8 to 15 leads to only a moderate improvement in the r.m.s. deviation of the fitted dipolar evolution function from 0.605 to 0.591. A further increase up to 113 points yields 0.583.

Again the moments of the distance distribution and also the widths $\Gamma_{0.5}$ and $\Gamma_{0.9}$ (Table 1) are reproduced best by the $P(r)$ obtained by Hermite polynomial

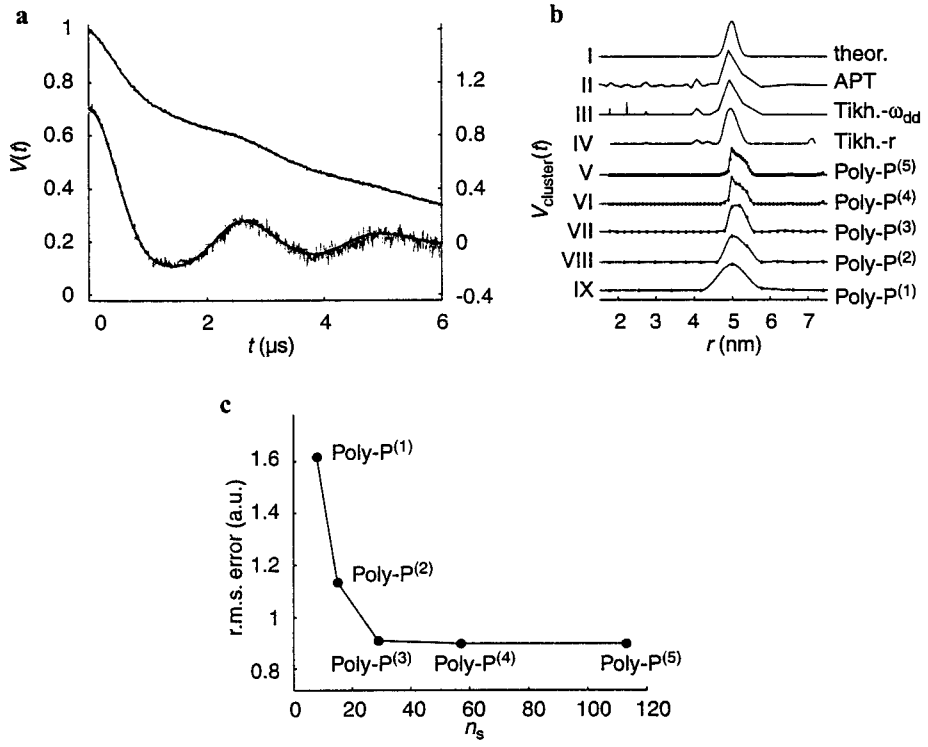

Fig. 2. Analysis of dipolar time evolution data with added noise for a model distance distribution consisting of one Gaussian peak at $r = 5$ nm with standard deviation $\sigma_r = 0.2$ nm. **a** Simulated dipolar time evolution function $V(t)$ (upper trace, left vertical scale) and cluster-only part $V_{\text{cluster}}(t)$ obtained by exponential background fitting (grey lower trace, right vertical scale). The black solid line in the lower trace is the best fit of a Hermite polynomial distance distribution function with 113 sampling points (Poly-$P^{(5)}$). **b** Distance distributions. I, model distribution used in simulating $V(t)$. II, distribution extracted by approximate Pake transformation. III, distribution extracted by Tikhonov regularization in dipolar frequency domain. IV, distribution extracted by Tikhonov regularization in distance domain. V–IX, distributions Poly-$P^{(n)}$ extracted by fitting Hermite polynomial distance distribution functions with different numbers of sampling points. Sampling points are marked by solid circles. **c** Dependence of the r.m.s. deviation between $V_{\text{cluster}}(t)$ and fitted dipolar evolution functions $V_{\text{fit}}(t)$ on the number of sampling points n_s.

fitting. Although the Poly-$P^{(n)}$ with a large number of sampling points clearly exhibit noise artefacts (see, e.g., Fig. 3b, trace IV), they provide characteristic parameters of the distribution that are close to the true values. Although the signal-to-noise ratio is lower for the data shown in Fig. 3c, $\langle r \rangle$, $\langle \Delta r^2 \rangle$, and $\Gamma_{0.5}$ could be determined with better precision than for the data shown in Fig. 3a. This can be traced back to the shorter time window. To substantiate this finding, we have simulated 100 dipolar evolution functions with the same mean square noise amplitude and same t_{max} as in Fig. 3c and analyzed them by Hermite polynomial fitting. We find that the mean distance $\langle r \rangle$ can be determined with a standard deviation of less than 0.015 nm, the second moment $\langle \Delta r^2 \rangle$ (variance)

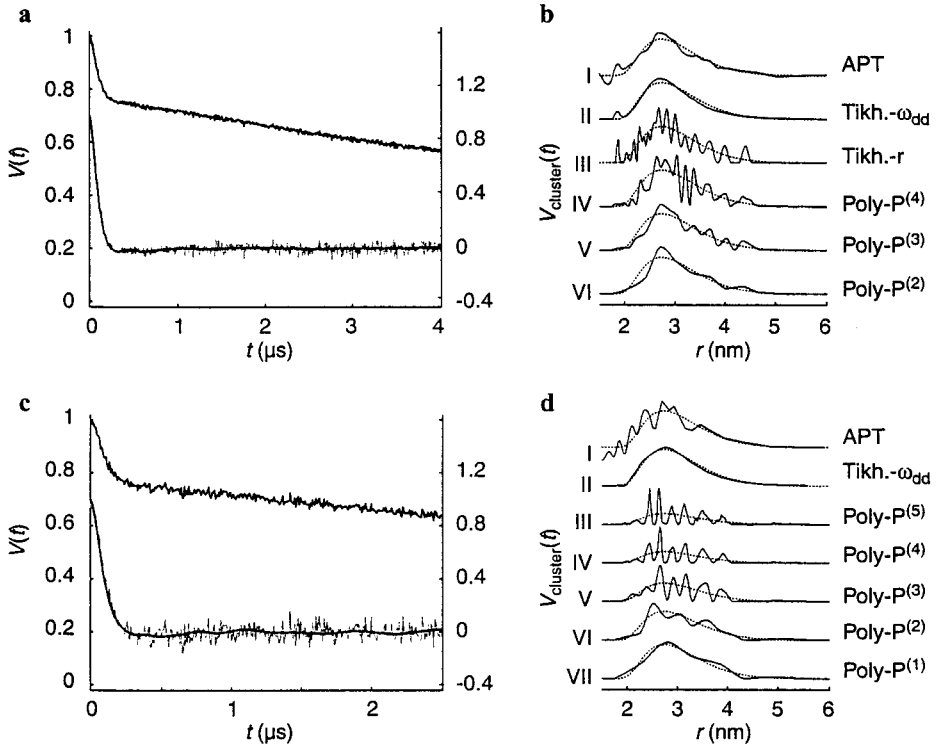

Fig. 3. Analysis of dipolar time evolution data with added noise for a model distance distribution consisting of a broad asymmetric Birnbaum-Saunders peak with $\mu = 1.4$ nm, $\beta = 1.45$ nm, $\gamma = 0.75$. **a** Simulated dipolar time evolution function $V(t)$ extending to $t_{max} = 4$ μs with moderate noise (upper trace, left vertical scale) and cluster-only part $V_{cluster}(t)$ obtained by exponential background fitting (grey lower trace, right vertical scale). The black solid line in the lower trace is the best fit of a Hermite polynomial distance distribution function with 29 sampling points (Poly-$P^{(3)}$). **b** Distance distributions extracted from $V_{cluster}(t)$ in **a** (solid lines) overlayed by the model distribution (dotted lines). I, distribution extracted by approximate Pake transformation. II, distribution extracted by Tikhonov regularization in dipolar frequency domain. III, distribution extracted by Tikhonov regularization in distance domain. IV–VI, distributions Poly-$P^{(n)}$ extracted by fitting Hermite polynomial distance distribution functions with different numbers of sampling points. **c** Simulated dipolar time evolution function $V(t)$ extending to $t_{max} = 2.5$ μs with strong noise (upper trace, left vertical scale) and cluster-only part $V_{cluster}(t)$ obtained by exponential background fitting (grey lower trace, right vertical scale). The black solid line in the lower trace is the best fit of a Hermite polynomial distance distribution function with 29 sampling points (Poly-$P^{(3)}$). **d** Distance distributions extracted from $V_{cluster}(t)$ in **c** (solid lines) overlayed by the model distribution (dotted lines). I, distribution extracted by approximate Pake transformation. II, distribution extracted by Tikhonov regularization in dipolar frequency domain. III–VII, distributions Poly-$P^{(n)}$ extracted by fitting Hermite polynomial distance distribution functions with different numbers of sampling points.

with a standard deviation of less than 0.02 nm^2, and $\Gamma_{0.5}$ with a standard deviation of less than 0.02 nm. The third moment $\langle \Delta r^3 \rangle$, which characterizes the asymmetry of the distribution, cannot be determined reliably by any of the data analysis procedures (Table 1).

Table 1. Characteristics of the asymmetric model distribution (see Fig. 3a, b) and errors of these characteristics for distributions reextracted by different analysis procedures from moderately noisy data.

Data analysis	% Deviation[a] from the following value of the model function				
	$\langle r \rangle$ = 3.042 nm	$\langle \Delta r^2 \rangle$ = 0.343 nm^2	$\langle \Delta r^3 \rangle$ = 0.169 nm^3	$\Gamma_{0.5}$ = 0.808 nm	$\Gamma_{0.9}$ = 1.803 nm
APT	−2.21	7.9	44.1	−5.2	6.6
Tikh.-ω_{dd}	−1.94	10.1	38.9	−8.8	7.6
Tikh.-r	−1.38	11.9	48.1	−3.4	12.0
Poly-$P^{(1)}$	0.89	5.7	−24.0	−9.1	14.2
Poly-$P^{(2)}$	1.20	−4.2	−19.5	−4.9	5.5
Poly-$P^{(3)}$	1.26	−3.9	−16.4	−4.8	3.1
Poly-$P^{(4)}$	1.25	−5.2	−24.0	−5.5	2.4
Poly-$P^{(5)}$	1.25	−4.7	−24.2	−5.2	2.1

[a] Deviations were calculated as $\Delta M_1/M_1$ for $\langle r \rangle$, $\Delta M_2/M_2$ for $\langle \Delta r^2 \rangle$, $\Delta M_3/M_3$ for $\langle \Delta r^3 \rangle$, $\Delta \Gamma_{0.5}/\Gamma_{0.5}$ for $\Gamma_{0.5}$, and $\Delta \Gamma_{0.9}/\Gamma_{0.9}$ for $\Gamma_{0.9}$.

Faithful extraction of distance distributions from dipolar evolution functions is expected to be most difficult in cases where the distribution contains both broad and narrow contributions. This is because then a regularization parameter or smoothing filter width cannot be optimum throughout the distribution. The problem is readily apparent for a model distribution consisting of three peaks with mean distances of 3, 4, and 5 nm and widths of 0.4, 0.5, and 0.2 nm, respectively (Fig. 4). Despite the fact that the signal-to-noise ratio is rather good in both traces, Tikhonov regularization in both frequency and distance domain runs into problems. With frequency domain Tikhonov regularization, the peak at 5 nm is completely missing (Fig. 4d, trace II, see arrow). Adaptive choice of the regularization parameter in distance domain Tikhonov regularization provides a too optimistic estimate of resolution. With Hermite polynomial fitting, the r.m.s. deviation for the data in Fig. 4a improves from 0.518 to 0.071 when increasing the number of sampling points from 8 to 57, while a further increase to $n_s = 113$ results in only an insignificant change of the r.m.s. deviation to 0.066. The best performance for these two data sets is obtained by APT. Indeed, the APT result can even be improved by zero filling (data not shown).

4.3 Peak Quantification in Model Data Sets

In some applications, it may be of interest to estimate the fractions of spin pairs that correspond to the peaks of a multimodal distance distribution. We have performed tests for a simple example of three baseline separated Gaussian peaks with widths of 0.2 nm (standard deviation) and mean distances of 2.25, 3.25, and 4.25 nm. The noise level (r.m.s. amplitude) was varied between 0.025 and

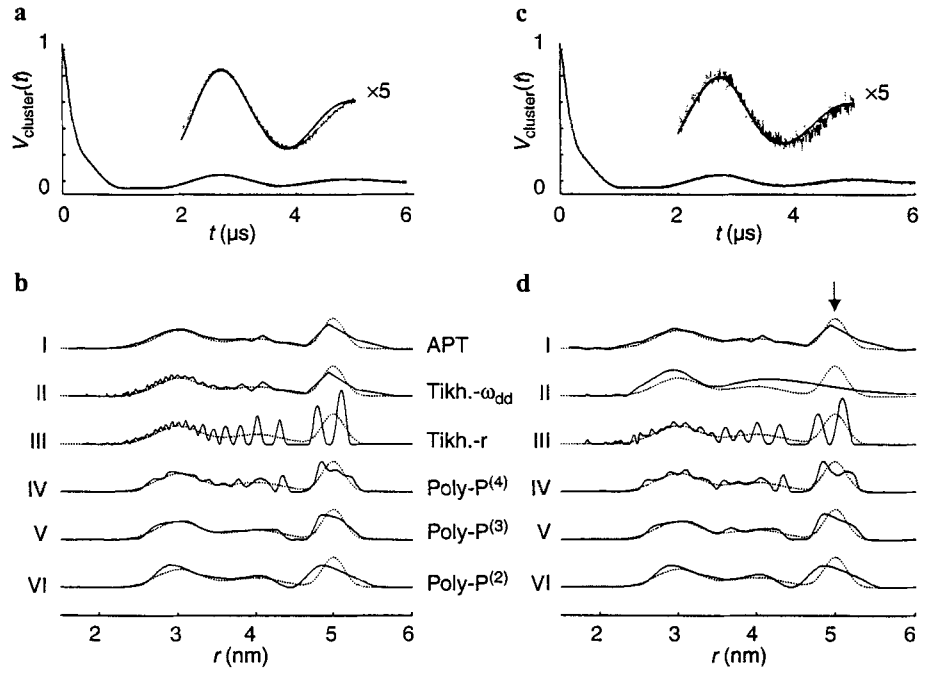

Fig. 4. Analysis of dipolar time evolution data with added noise for a model distance distribution consisting of three Gaussian peaks at $r_1 = 3$ nm (standard deviation $\sigma_{r1} = 0.4$ nm), $r_2 = 4$ nm ($\sigma_{r2} = 0.5$ nm), and $r_3 = 5$ nm ($\sigma_{r2} = 0.2$ nm). For labeling of distribution functions in **b** and **d** see Fig. 3. **a** Simulated cluster-only part $V_{cluster}(t)$ (grey line) with low noise and best fit of a Hermite polynomial distance distribution function with 29 sampling points (Poly-$P^{(3)}$). The inset shows the range $t = 2$–5 μs with five times increased amplitude. **b** Distance distributions extracted from $V_{cluster}(t)$ in **a** (solid lines) overlayed by the model distribution (dotted lines). **c** Simulated cluster-only part $V_{cluster}(t)$ (grey line) with moderate noise and best fit of a Hermite polynomial distance distribution function with 29 sampling points (Poly-$P^{(3)}$). The inset shows the range $t = 2$–5 μs with five times increased amplitude. **d** Distance distributions extracted from $V_{cluster}(t)$ in **c** (solid lines) overlayed by the model distribution (dotted lines). The arrow designates the peak at 5 nm that is missing in distance domain Tikhonov regularization.

0.8% of the total echo amplitude and a modulation depth $\lambda = 0.16$ was assumed. The dependence of the sum of the standard deviations of all three peak amplitudes on the noise level is displayed in Fig. 5 for the different data analysis procedures. It is apparent that distance domain Tikhonov regularization performs best for this task. If the signal-to-noise ratio is decreased by another factor of two (1.6% r.m.s. noise amplitude, data not shown) the determination of the optimum regularization parameter in the FTIKREG algorithm fails. However, for such low-noise data, quantification by any of the other methods is not reliable either. Up to approximately 0.5% r.m.s. noise, APT and Hermite polynomial fitting with a sufficiently large number of sampling points (Poly-$P^{(5)}$) also provide satisfying results.

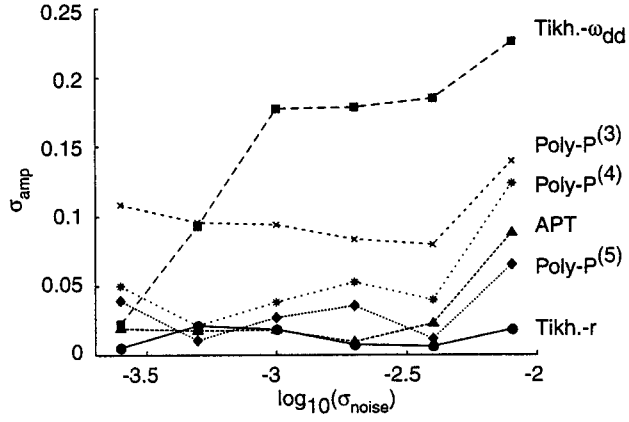

Fig. 5. Standard deviation σ_{amp} of the three peak intensities in a model distribution with three narrow peaks ($r_1 = 2.25$ nm, $r_2 = 3.25$ nm, $r_3 = 4.25$ nm, $\sigma_{r1} = \sigma_{r2} = \sigma_{r3} = 0.2$ nm) as a function of the amplitude σ_{noise} of white noise for different data analysis procedures. For labelling of the procedures see Fig. 3.

4.4 Extraction of Distance Distributions from Experimental Data Sets

In experimental data sets, complications beyond the presence of white noise may be encountered. For instance, nuclear modulations are not completely suppressed in the four-pulse DEER experiment and may give rise to an artefact at about 1.5 nm at X-band frequencies of about 9.6 GHz [13]. As can be seen for the example of a shape-persistent biradical with a spin-to-spin distance of about 5 nm [25], this artefact is well confined in frequency domain Tikhonov regularization (see arrow in Fig. 6b) and has a tolerable influence in APT analysis. Distance domain Tikhonov regularization and Hermite polynomial fitting can be restricted to the distance range at which the data are reliable.

Apart from this, the quality of the results for Hermite polynomial fitting and APT is similar to the quality obtained for simulated data (compare Figs. 2 and 6). Somewhat surprisingly, this is not true for distance domain Tikhonov regularization (Fig. 6, trace III). Probably the difficulty in extracting the optimum regularization parameter is due to slightly stronger noise combined with nuclear modulation and deviations from the ideal dipolar evolution function caused by orientation selection [19]. Moment analysis of the Hermite polynomial fit Poly-$P^{(5)}$ gives a mean distance of 5.02 nm and a width $\Gamma_{0.5}$ of 0.19 nm in good agreement with previous results for this biradical [16, 17].

In recent work on the characterization of the coconformation of [2]catenanes, we encountered broad asymmetric distance distributions [6]. For a shock-frozen chloroform solution, we found that the primary data could be simulated quite well by a simple geometric model for the two concatenated macrocycles. This was not true, however, for the same compounds in glassy *o*-terphenyl. A model-free

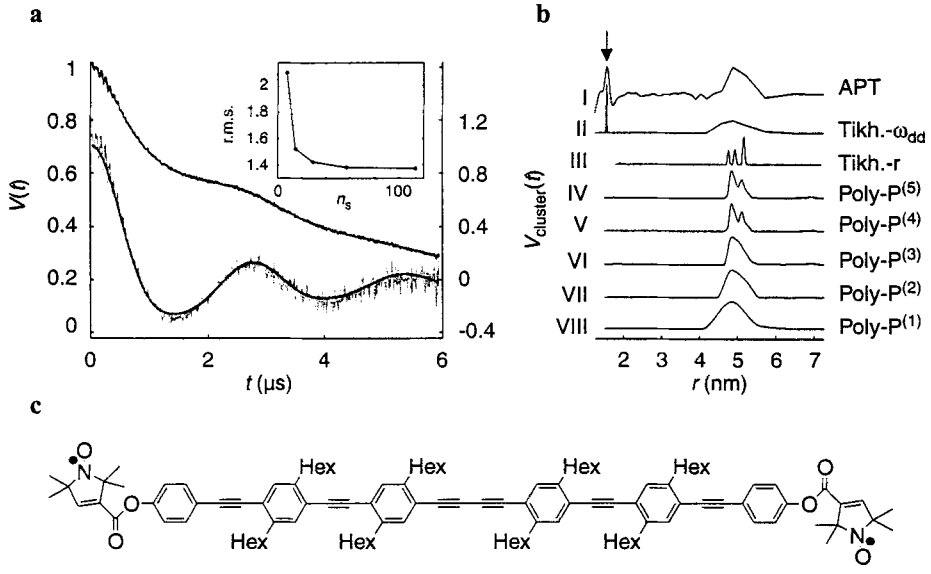

Fig. 6. Analysis of experimental dipolar time evolution data for a shape-persistent biradical with an end-to-end distance of approximately 5 nm. **a** Primary experimental data normalized at $t = 0$ (upper trace) and cluster-only part $V_{cluster}(t)$ obtained by exponential background fitting (grey lower trace, right vertical scale). The black solid line in the lower trace is the best fit of a Hermite polynomial distance distribution function with 113 sampling points (Poly-$P^{(5)}$). The inset shows the dependence of the r.m.s. deviation of $V_{fit}(t)$ from $V_{cluster}(t)$ on the number of sampling points n_s used in polynomial fitting. **b** Distance distributions extracted from $V_{cluster}(t)$ in **a** (solid lines) by different data analysis techniques (for labelling see Fig. 3). The arrow marks an artefact at 1.5 nm caused by residual proton modulation of the signal. **c** Structure of the biradical.

quantification of such broad asymmetric distributions would thus be of considerable interest. As can be seen in Fig. 7, distance distributions extracted by different data analysis procedures differ considerably from each other for this case. Estimation of the optimum regularization parameter in distance domain Tikhonov regularization fails (Fig. 7b, trace III), while frequency domain Tikhonov regularization produces a reasonable result. Some of the problems can be traced back to the fact that $V_{cluster}(t)$ has not completely decayed, which makes separation of this contribution from the homogeneous background difficult. Moment analysis shows that the different distance distributions, with the exception of the one obtained by APT, agree reasonably well in some characteristics. Mean distances range between 3.2 and 3.8 nm, first moments between 1.0 and 1.3 nm^2, $\Gamma_{0.5}$ between 1.6 and 1.9 nm, and $\Gamma_{0.9}$ between 2.9 and 3.3 nm.

For the double mutant S106C/S160Ch of LHCII reconstituted with lutein as the xanthophyll component, the distance distribution is considerably narrower than that for the [2]catenane (Fig. 8). Consequently, differences between the results of the alternative data analysis procedures are less dramatic (Table 2). Moment analysis of the distributions from all the different analysis procedures consistently

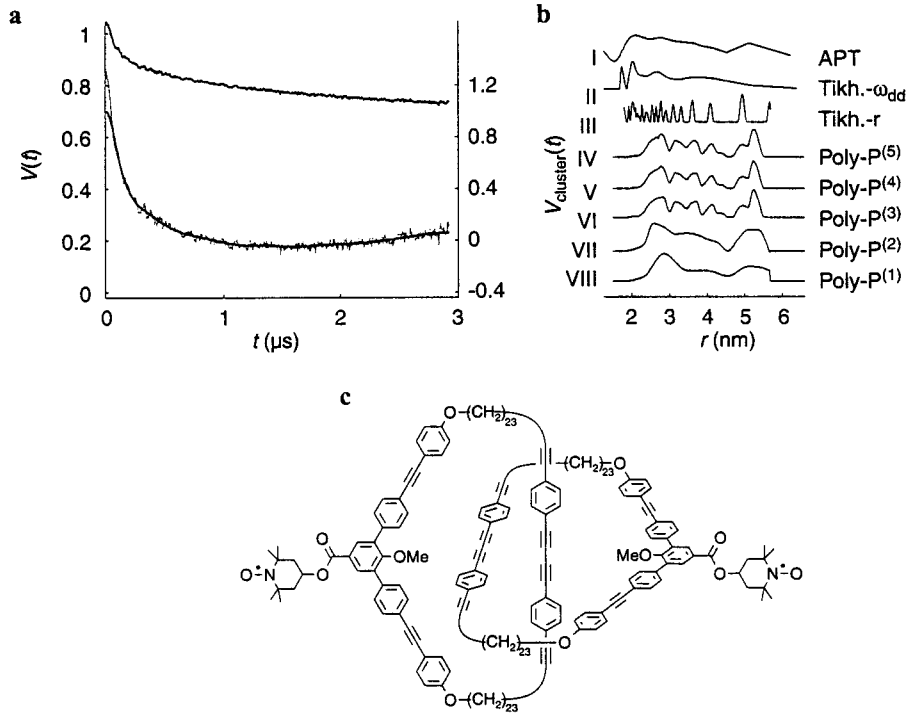

Fig. 7. Analysis of experimental dipolar time evolution data for a doubly labelled medium-sized [2]catenane with a broad distribution of spin-to-spin distances [6]. **a** Primary experimental data normalized at $t = 0$ (upper trace) and cluster-only part $V_{cluster}(t)$ obtained by exponential background fitting (grey lower trace, right vertical scale). The black solid line in the lower trace is the best fit of a Hermite polynomial distance distribution function with 29 sampling points (Poly-$P^{(3)}$). **b** Distance distributions extracted from $V_{cluster}(t)$ in **a** by different data analysis techniques (for labelling see Fig. 3). To the result of approximate Pake transformation a distance domain smoothing with a filter width of 0.25 nm was applied. **c** Structure of the doubly labelled [2]catenane.

results in mean distances $\langle r \rangle = 4.0$–4.15 nm and widths $\Gamma_{0.5} = 1.0$–1.4 nm. Similar ranges of $\langle r \rangle = 3.85$–4.15 nm and $\Gamma_{0.5} = 0.9$–1.3 nm are obtained for both measurements (see Fig. 2a) of the same double mutant of LHCII reconstituted with ZX. In the latter case, results with APT have been excluded. Results for LHCII reconstituted with NX are in the ranges $\langle r \rangle = 3.9$–4.25 nm and $\Gamma_{0.5} = 1.15$–1.6 nm (again APT excluded). There is some indication for an increase in the mean distance and in the width of the distribution for NX, but on the basis of these values it can hardly be claimed that the difference is statistically significant. However, the second moment of the distance distribution $\langle \Delta r^2 \rangle$ is consistently larger for NX compared to lutein and ZX (see also Table 2). This is in agreement with the broadening of the distance distribution for NX compared to ZX that is indicated by direct comparison of the primary data.

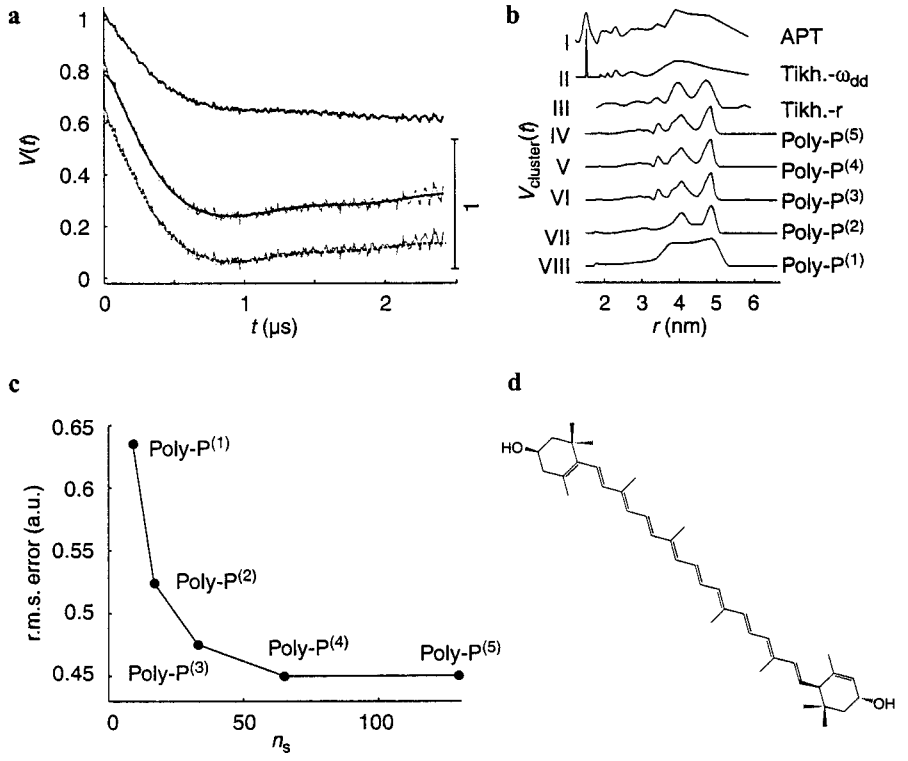

Fig. 8. Analysis of experimental dipolar time evolution data for the the doubly spin-labelled double mutant S106C/S160Ch of LHCII reconstituted with lutein as the xanthophyll component. **a** Primary experimental data normalized at $t = 0$ (upper trace) and cluster-only part $V_{cluster}(t)$ obtained by exponential background fitting (grey lower traces, right vertical amplitude ruler). The black solid lines in the two lower traces are the best fits of a Hermite polynomial distance distribution function with 113 sampling points (Poly-$P^{(5)}$, medium trace) and by distance domain Tikhonov regularization (Tikh.-r, lowest trace). **b** Distance distributions extracted from $V_{cluster}(t)$ in **a** by different data analysis techniques (for labelling see Fig. 3). **c** Dependence of the r.m.s. deviation between $V_{cluster}(t)$ and fitted dipolar evolution functions $V_{fit}(t)$ on the number of sampling points n_s. **d** Structure of lutein.

Table 2. Characteristics of the label-to-label distance distribution Poly-$P^{(5)}$ of the double mutant S106C/S160Ch of LHCII reconstituted with different pure xanthophyll components. For zeaxanthin and neoxanthin, two preparations each were measured.

Characteristics	$\langle r \rangle$ (nm)	$\langle \Delta r^2 \rangle$ (nm^2)	$\langle \Delta r^3 \rangle$ (nm^3)	$\Gamma_{0.5}$ (nm)	$\Gamma_{0.9}$ (nm)
Lutein	4.14	0.424	−0.211	1.07	2.05
Zeaxanthin(1)	4.13	0.406	−0.175	0.99	2.06
Zeaxanthin(2)	4.14	0.436	−0.231	1.12	2.03
Neoxanthin(1)	4.24	0.493	−0.250	1.10	1.92
Neoxanthin(2)	4.17	0.525	−0.250	1.17	2.25

5 Discussion

Clearly, none of the alternative approaches for extracting $P(r)$ from background-corrected dipolar evolution data $V_{cluster}(t)$ consistently provides reliable results. It is therefore highly advisable to select the data analysis procedure that is best suited to the problem at hand and to cross-check the results. Model-free extraction of broad distance distributions may only be possible if the expected resolution in distance domain is known in advance. Otherwise, such distributions should be characterized by their mean value and variance.

If the distance distribution consists of only narrow peaks (widths of a few tenths of a nanometer), all data analysis procedures provide reliable results. In this case, the best resolution and least influence of noise on the result is obtained by distance domain Tikhonov regularization. If the distance distribution consists only of broad contributions (width of the most narrow feature larger than 1 nm), distance domain Tikhonov regularization tends to fail, while all the other methods give reasonable results. In this situation the most faithful result for $P(r)$ tends to be obtained by frequency domain Tikhonov regularization. However, if moment analysis of the distribution is intended, better results are obtained with Hermite polynomial fitting with a large number of sampling points. Distance distributions consisting of both narrow and broad peaks are the most complicated case. Adaptive choice of the regularization parameter for Tikhonov regularization then tends to fail in both distance and frequency domain. Such data are better analyzed by approximate Pake transformation or Hermite polynomial fitting, provided that the signal-to-noise ratio is good.

Generally, the quality of experimental data is characterized by the signal-to-noise ratio and the maximum dipolar evolution time t_{max}. For the currently used constant-time evolution experiments these two characteristics are strongly interdependent and a compromise between them must be made before the measurement. Work on an alternative approach on the basis of the four-pulse DEER experiment is in progress. The choice of t_{max} decides to what extent the homogeneous background contribution from remote spins can be eliminated from the data. Admixture of part of this contribution to $V_{cluster}(t)$ causes errors in the extracted distance distribution mainly at the upper end of the distance range (see trace IV in Fig. 2b and all the traces in Fig. 7b). This in turn influences moment analysis. For this reason, moment analysis for the experimental data of the [2]catenane is less precise than would be expected from the results for the asymmetric Birnbaum-Saunders model distribution (Table 1). Analysis of these model data also indicates that using unnecessarily long t_{max} leads to a decrease of the reliability of moment analysis. Ideally, t_{max} should be just sufficient to obtain a reliable fit of the background contribution. Moment analysis of APT data can lead to poor results as the constraint $P(r) \geq 0$ is lacking.

Limited signal-to-noise ratio can be compensated rather well by Tikhonov regularization techniques if the distance distribution consists of only narrow or only broad peaks. If both narrow and broad features occur, none of the techniques is expected to extract a reliable distance distribution from noisy data. In

this situation, an appropriate value of t_{max} should be selected on the basis of preliminary data and high-quality final data should then be measured under carefully optimized conditions (see also [18]). If this still does not provide data of sufficient quality for a direct analysis, it may still be possible to discuss changes in distance distributions in a series of samples by comparison of data sets after renormalization of the modulation depth by the optimum factor f_λ.

Appendix

Kernel function for the Tikhonov regularization program FTIKREG dipolar frequency domain:

```
DOUBLE PRECISION FUNCTION KTISJ1(T,S)
   IMPLICIT NONE
   DOUBLE PRECISION T,S,X,PI,SUM,WDD,WAC
   INTEGER I
   PI=3.141592654
   WDD=2.*PI*S
   SUM=0.
   DO 10 I=1,1000
     X=I/1000.0
     WAC=WDD*(3*X*X-1)
     SUM=SUM+DCOS(WAC*T)
10 CONTINUE
   KTISJ1=SUM
   RETURN
   END
```

Kernel function for the Tikhonov regularization program FTIKREG distance domain:

```
DOUBLE PRECISION FUNCTION KTISJ1(T,S)
   IMPLICIT NONE
   DOUBLE PRECISION T,S,X,PI,SUM,WDD,WAC,NY0,R3
   INTEGER I
   PI=3.141592654
   NY0=52.04
   R3=*S*S*S
   WDD=2.*PI*NY0/R3
   SUM=0.
   DO 10 I=1,1000
     X=I/1000.0
     WAC=WDD*(3*X*X-1)
     SUM=SUM+DCOS(WAC*T)
10 CONTINUE
   KTISJ1=SUM
   RETURN
   END
```

Acknowledgements

We thank T. Roths and J. Honerkamp from Freiburger Materialforschungszentrum for kindly providing the source code of the program FTIKREG for Tikhonov regularization.

References

1. Schweiger A., Jeschke G.: Principles of Pulse Electron Paramagnetic Resonance. Oxford: Oxford University Press 2001.
2. Berliner L.J., Eaton S.S.: Biological Magnetic Resonance (Eaton G.R., ed.), vol. 19. New York: Plenum 2000.
3. Jeschke G.: Macromol. Rapid Commun. **23**, 227 (2002)
4. Pannier M., Schädler V., Schöps M., Wiesner U., Jeschke G., Spiess H.W.: Macromolecules **33**, 7812 (2000)
5. Pannier M., Schöps M., Schädler V., Wiesner U., Jeschke G., Spiess H.W.: Macromolecules **34**, 5555 (2001)
6. Jeschke G., Godt A.: Chem. Phys. Chem. **4**, 1328 (2003)
7. Hubbell W.L., Cafiso D.S., Altenbach C.: Nat. Struct. Biol. **7**, 735 (2000)
8. Hubbell W.L., Altenbach C., Hubbell C.M., Khorana H.G.: Trends Biochem. Sci. **27**, 288 (2003)
9. Borbat P.P., Freed J.H.: J. Am. Chem. Soc. **124**, 5304 (2002)
10. Milov A.D., Salikhov K.M., Shirov M.D.: Fiz. Tverd. Tela (Leningrad) **23**, 957 (1981)
11. Milov A.D., Ponomarev A.B., Tsvetkov Yu.D.: Chem. Phys. Lett. **110**, 67 (1984)
12. Milov A.D., Maryasov A.G., Tsvetkov Yu.D.: Appl. Magn. Reson. **15**, 107 (1998)
13. Pannier M., Veit S., Godt A., Jeschke G., Spiess H.W.: J. Magn. Reson. **142**, 331 (2000)
14. Kurshev V.V., Raitsimring A.M., Tsvetkov Yu.D.: J. Magn. Reson. **81**, 441 (1989)
15. Borbat P.P., Freed J.H.: Chem. Phys. Lett. **313**, 145 (1999)
16. Jeschke G., Pannier M., Godt A., Spiess H.W.: Chem. Phys. Lett. **331**, 243 (2000)
17. Jeschke G., Koch A., Jonas U., Godt A.: J. Magn. Reson. **155**, 72 (2001)
18. Jeschke G.: Chem. Phys. Chem. **3**, 927 (2002)
19. Larsen R.G., Singel D.J.: J. Chem. Phys. **98**, 5134 (1993)
20. Milov A.D., Samoilova R.I., Tsvetkov Yu.D., Gusev V.A., Formaggio F., Crisma M., Toniolo C., Raap J.: Appl. Magn. Reson. **23**, 81 (2002)
21. Milov A.D., Tsvetkov Yu.D., Gorbunova E.Y., Mustaeva L.G., Ovchinnikova T.V., Raap J.: Biopolymers **64**, 328 (2002)
22. Tikhonov A.N., Arsenin V.Y. in: Solutions of Ill-Posed Problems. New York: Wiley 1977.
23. Honerkamp J., Weese J.: Contin. Mech. Thermodin. **2**, 17 (1990)
24. Weese J.: Comput. Phys. Commun. **69**, 99 (1992)
25. Godt A., Franzen C., Veit S., Enkelmann V., Pannier M., Jeschke G.: J. Org. Chem. **65**, 7575 (2000)
26. Duda S., Godt A.: Eur. J. Org. Chem. **2003**, 3412.
27. Paulsen H., Finkenzeller B., Kühlein N.: Eur. J. Biochem. **215**, 809 (1993)
28. Vogt F.G., Aurentz D.J., Mueller K.T.: Mol. Phys. **95**, 907 (1998)
29. Steinhoff H.J., Suess B.: Methods **29**, 188 (2003)
30. Birnbaum Z.W., Saunders S.C.: J. Appl. Probab. **6**, 319 (1969)

Authors' address: Gunnar Jeschke, Max Planck Institute for Polymer Research, Postfach 3148, 55021 Mainz, Germany
E-mail: jeschke@mpip-mainz.mpg.de